Journal of Environmental Management 207 (2018) 387–395

Contents lists available at ScienceDirect

Journal of Environmental Management

journal homepage: www.elsevier.com/locate/jenvman

Research article

A novel Fe-La-Ce tri-metallic composite for the removal of fluoride ions from aqueous media

S.K.T. Thathsara, P.L.A.T. Cooray, Thilini Kuruwita Mudiyanselage, Nilwala Kottegoda, Dilru R. Ratnaweera*

Department of Chemistry, Faculty of Applied Sciences, University of Sri Jayewardenepura, Gangodawila, Nugegoda, Sri Lanka

ARTICLE INFO

Article history:
Received 13 July 2017
Received in revised form
14 October 2017
Accepted 15 November 2017

Keywords:
Tri-metallic composite
Adsorption isotherms
fluoride removal
Adsorption kinetics

1. Introduction

Fluoride is a ubiquitous anion present in natural waters. Higher amounts of fluorides in drinking water sources have been reported in many Asian and African countries, including Sri Lanka, India, China and Ghana (Güler and Thyne, 2004). The beneficial and detrimental effects of fluoride on human health are already well known. Even though fluoride is an indispensable micro-nutrient which expended on strengthening of bones and tooth, an exorbitant amount of fluoride is harmful, and could cause fluorosis (dental, skeletal and crippling), osteoporosis, arthritis, brittle bones, cancer, infertility, brain damage, Alzheimer syndrome, and thyroid disorder (Naim et al., 2012). Even though the World Health Organization marks the general upper limit of fluoride ions in drinking water as 1.5 mg/L, the generally recommended maximum fluoride concentration is 1.0 mg/L for tropical countries, due to higher consumption of water when compared to other countries (Yu et al., 2015a). Fluoride levels in surface water have been increased during the last few decades in many water resources across the globe, to the point where immediate attention is needed in order to minimize the fluoride contamination and to introduce efficient fluoride removing techniques to the public. Weathering of fluoride containing minerals and industrial discharges are the major reasons for the fluoride hikes in surface water (Wei et al., 2016).

Numerous attempts have been reported on implementing economical and efficient new technologies, for the removal of excess fluoride from drinking-water resources. Adsorption (Bhatnagar et al., 2011; Dong and Wang, 2016; Noorjahan et al., 2015), ion exchange (Yu et al., 2015b), chemical precipitation (Gogoi et al., 2015), membrane filtration (Choi et al., 2001; Oshima et al., 1996), reverse osmosis (Sehn, 2008) and electrodialysis (Ergun et al., 2008) are the most commonly used methods in the current process of water purification. The method of adsorption has been identified as the most promising due to its simplicity in application and economic feasibility. Adsorption based fluoride removers have utilized many fluoride adsorbents such as ion (Yu et al., 2015b), aluminum (Rafique et al., 2013), calcium (Turner et al., 2005), clay (Tor, 2006), activated carbon and alumina (Daifullah et al., 2007; Rafique et al., 2012), and agricultural and industrial waste (Cai et al., 2015; Ganvir and Das, 2011; Prabhu and Meenakshi, 2015). However, the low efficiency of these adsorbates still is the main problem.

Recent developments of the relevant studies have focused on adsorbents containing rare earth metals such as La, Ce and Zr that possess an inherent strong affinity toward fluoride (Prabhu and Meenakshi, 2015). In addition to that, some studies have demonstrated that metal composites with rare earth metals such as Fe-Al-Ce (Chen et al., 2009), Fe-Zr (Biswas et al., 2007), Mg-La-Ce (Wu et al., 2016), Fe-Mg-La (Yu et al., 2015a), Ca-Al-La (Xiang et al., 2014), and Fe-Mg-Al (Ma et al., 2011) would maintain a high fluoride adsorption capacity at a lower cost. However, systematic studies of selecting proper metal combinations and compositions have not been reported so far.

This study highlights a systematic way of selecting and formulating a novel tri-metal composite for fluoride removal and elaborates experimental evidence for the ability of fluoride-metal complexation. Metal and metal hydroxides with high affinity toward fluoride ions were selected from related literature (Bhatnagar et al., 2011) and tri-metal combinations were tested for their absorption capacity. This study discusses the preparation,

* Corresponding author.
E-mail address: dilru@sci.sjp.ac.lk (D.R. Ratnaweera).

https://doi.org/10.1016/j.jenvman.2017.11.041
0301-4797/© 2017 Elsevier Ltd. All rights reserved.

characterization and efficiency of fluoride ion removal of the Fe-La-Ce tri-metal composite as an effective remedy for the removal of excess fluoride in aqueous media. Tri-metal composite was synthesized, following the one step co-precipitation method reported (Yu et al., 2015a). The batch adsorption experiments were carried out to study and investigate adsorption kinetics and adsorption isotherms.

2. Methodology

2.1. Materials

All chemicals and reagents ($LaCl_3 \cdot 7H_2O$, $FeSO_4.7H_2O$, $Ce(SO_4)_2 \cdot 4H_2O$, NaOH and NaF) were obtained from analytical grade and were purchased from Sigma Aldrich. 10000 mg/L standard fluoride solution was purchased from WTW. Working fluoride solutions were prepared freshly by diluting 10000 mg/L stock solution with deionized water. Nylon membrane (0.45 μm) and Whatman 41 filter papers were used for filtration purposes.

2.2. Preparation of tri-metallic composite

Metal solutions with 1:1:1 mole ratios were prepared using 0.10 mol dm^{-3} individual metal ($LaCl_3 \cdot 7H_2O$, $FeSO_4.7H_2O$ and $Ce(SO_4)_2 \cdot 4H_2O$) stock solutions. The co-precipitation of metal mixtures was achieved by adjusting pH to 8.5 using a 6 mol dm^{-3} NaOH solution while stirring continuously. Precipitates were filtered and washed with deionized water until the pH of the filtrate reached 6.5 ± 0.2. Oven dried precipitates were sieved using 500 μm sieves.

2.3. Characterization of tri-metallic composite

Fourier Transform Infrared spectroscopy (FTIR) was used to characterize Fe-La-Ce adsorbate before and after having been exposed to fluoride ions. Optical grade KBr pellet was used for background corrections. FTIR measurements were carried out using Nicolet IS 10 instrument from 500 to 4000 cm^{-1} wavenumber range.

Further characterization of the Fe-La-Ce tri-metal composite was done through the powder X-ray diffraction technique. XRD peak analysis of a mixture of metal compounds is a challenging task. In order to surmount that, XRD patterns of the starting materials were also obtained and compared with the XRD peak positions of the metal compounds in the composite sample. The XRD measurements were carried out using (Rigaku, Ultima IV instrument) Cu Kα radiation (λ = 1.54 Å) over 2θ range of 2° to 70° with a step size of 0.02° for above samples.

The elemental compositions of above tri-metal composites were studied using a HORIBA Scientific XGT-5200 X-ray Fluorescence (XRF) instrument and corresponding peak analysis were done using the HORRIBA X-ray analytical microscope software.

Surface morphology of pristine adsorbate and adsorbate treated with fluoride ions were studied using Hitachi SU6600 SEM with an acceleration voltage of 15.0 kV. Observations were conducted in the secondary electron mode.

The point of zero charge (PZC) was calculated using a procedure reported by Yu et al. (2015a). 0.01 M $NaNO_3$ solution (50 mL) was added to a known weight of tri-metallic composite and the mixture was shaken for 24 h. Then the pH of the suspension was adjusted to various pH values using 0.1 M NaOH and HNO_3. The suspension was stirred further for 60 min until equilibrium was attained. Then the initial pH of the solution was measured using a pH meter (OHAUS starter 3000). Finally, 1.5 g of $NaNO_3$ was added to the suspension and stirred for 3 h and final pH of the sample was measured. The PZC was calculated by plotting ΔpH (final pH − initial pH) against final pH. The PZC is the pH at which ΔpH = 0 (Cristiano et al., 2011).

2.4. Adsorption studies

2.4.1. Effect of contact time

All adsorption experiments were conducted in 100 ml volume of test solutions and the mass of the sorbent used in each study was 0.01 g. A known weight (0.01 g) of Fe-La-Ce tri-metallic composite was added into 250 ml polypropylene plastic bottle containing 100 mL of 10 mg/L fluoride solution. Above mixture was placed on a shaker (Clifton shaker) for different time intervals at a constant speed (200 rpm) at 300 K. A known volume (1 mL) of fluoride solution was withdrawn from the above mixture every 60 min. The withdraw solutions were filtered using 0.45 μm nylon filter and the residual fluoride concentration of the filtrate were measured using a fluoride selective electrode (WTW F800) connected to a multi-ion meter (WTW pH/ion 340i). Calibration of the instrument was done according to the instructions provided by the instrument manufacturer using a WTW 140100 TISAB solution. The weight of the fluoride ions adsorbed per unit weight of adsorbent (mg/g) was calculated according to equation (1).

$$q_e = \frac{(C_0 - C_e)}{m} \times V \tag{1}$$

$$Removal\ efficiency\ \% = \frac{C_0 - C_e}{C_0} \times 100 \tag{2}$$

where, m is the weight of the adsorbent in grams, q_e (mg/g) is the amount of fluoride adsorbed per unit weight of the adsorbent, C_0 (mg/L) is the initial concentration of fluoride ions, C_e (mg/L) is the final concentration of fluoride ions, V (L) is the volume of the solution.

2.4.2. Effect of pH

Fluoride solution with initial concentration of 10 mg/L was used to determine the effect of pH on fluoride ions adsorption. Adsorbent dose of 0.1 g/L was used to carry out this experiment. HNO_3 and NaOH were added to adjust the pH of the medium during the fluoride ions adsorption process. Medium pH was measured using a pH meter (OHAUS starter 3000). At the end of each sorption process, the samples were filtered through 0.45 μm nylon filter. Fluoride concentrations were determined using a fluoride meter as described above. The amount of fluoride ions adsorbed per unit weight of adsorbent (mg/g) was calculated using the same procedure mentioned in section 2.4.1.

2.4.3. Effect of initial concentration

Series of 10–100 mg/L of fluoride solutions were prepared at pH 7.00 ± 0.01. These, fluoride concentration series were treated using tri-metallic composite at 300 K (Favier et al., 2016). After 2 h, the residual fluoride concentration was measured. Finally, the amount of fluoride ion adsorbed per unit weight of adsorbent (mg/g) was calculated using the same procedure mentioned in section 2.4.1.

2.4.4. Effect of competitive factors

Different concentrations (0.100 M, 0.010 M and 0.001 M) of NaCl, Na_2SO_4 and $NaHCO_3$ solutions were introduced into the 10 mg/L of standardized fluoride solution. All solutions were kept at 300 K in pH 7 for 2 h while moving at a speed of 200 rpm. Then fluoride adsorption capacities of tri-metal composites were analyzed using the fluoride selective electrode method described previously in section 2.4.1.

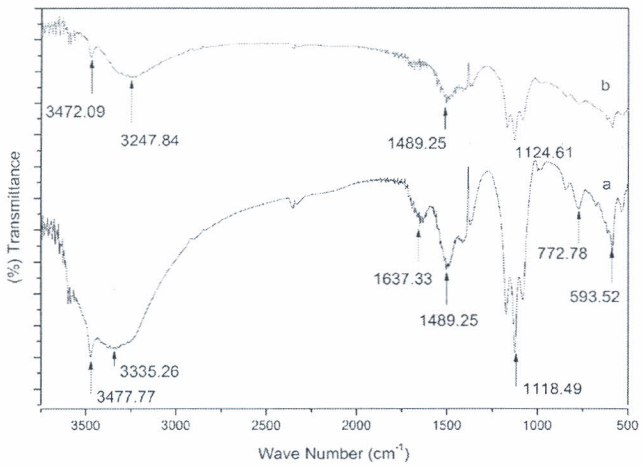


Fig. 1. FTIR spectra for (a) before and (b) after fluoride adsorb onto the Fe-La-Ce tri-metallic composite.

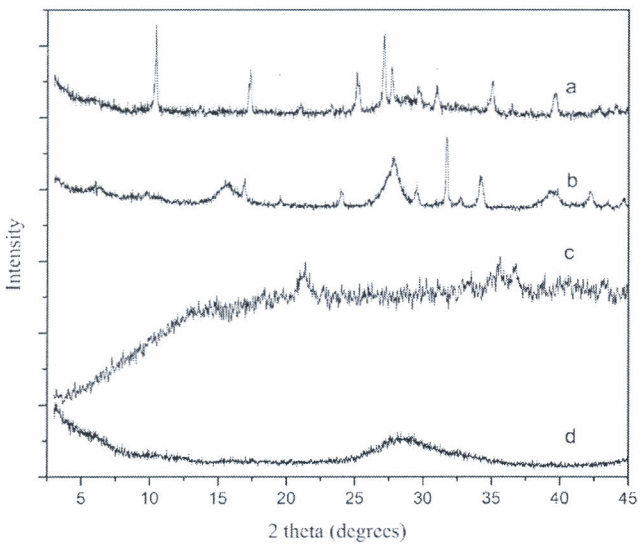


Fig. 2. XRD patterns of (a) Fe-La-Ce tri-metal composite, (b) $La(OH)_3$, (c) FeO(OH) and (d) $Ce(OH)_3$.

2.4.5. Adsorption isotherms

Concentration series of 10–100 mg/L of fluoride solutions were prepared at pH 4.00 ± 0.01 and 7.00 ± 0.01. This experiment was conducted at different temperatures (300 K, 310 K, 320 K and 330 K). A known weight (X g) of trimetal adsorbent was introduced into the fluoride solutions. After 2 h, residual fluoride concentrations were calculated using the method mentioned in section 2.4.1. Collected data were fitted to Langmuir and Freundlich adsorption isotherms.

2.4.6. Adsorption kinetics

Standard fluoride solutions having concentrations in between 10 mg/L to 50 mg/L were treated with 0.1 g/L of tri-metal adsorbent while shaking at a constant speed of 200 rpm. Treated solutions were filtered using 0.45 μm nylon filters and the remaining fluoride concentrations were determined using a fluoride meter as a function of contact time. Resulting data were analyzed using pseudo-first order and pseudo-second order rate laws.

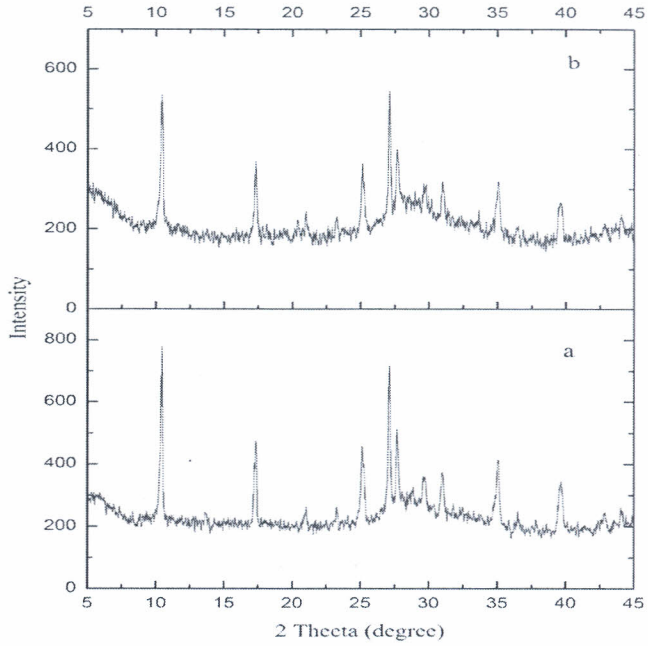


Fig. 3. XRD spectra of (a) virgin tri-metal composite and (b) fluoride treated tri-metal composite.

Table 1
The XRF analysis of metal compositions of tri-metal adsorbent before and after fluoride adsorbed onto Fe-La-Ce tri-metallic composite.

Element	Mole % of Metals	
	Pristine adsorbent	After fluoride adsorbed onto Fe-La-Ce composite
Fe	33.21 ± 0.21	28.98 ± 0.16
La	29.88 ± 0.41	28.10 ± 0.32
Ce	28.01 ± 0.41	30.04 ± 0.35

2.4.7. Regeneration study

A known weight of adsorbent (0.10 g) was added into 100.00 mL of 10.00 mg/L sodium fluoride solution and gently shaken for 2 h using a Clifton Shaker at 200 rpm. Then the adsorbent was separated from the solution by filtration and dried at 28 °C. These collected dried adsorbent was added into 100.00 mL of 0.1 M NaOH solution while stirring for 2 h to remove the adsorbed fluoride from the tri-metal composite. The concentration of the desorbed fluoride was calculated using the method mentioned in section 2.4.1. Then the de-fluoridated adsorbent was collected and washed using deionized water until pH of the filtrate reached 7.00 ± 0.5. It was dried at 300 K for 5 h.

3. Results and discussion

3.1. Characterization

3.1.1. Fourier Transform Infrared spectroscopy (FTIR)

Fig. 1 shows the FTIR spectra of virgin and fluoride adsorbed tri-metal adsorbents. The peaks around 3477 cm^{-1} and 1637 cm^{-1} are due to stretching and bending vibration of adsorbed H_2O on the surface of Fe-La-Ce tri-metallic composite (Zhang et al., 2005). The intense narrow peak at 1489 cm^{-1} indicates the presence of carbonate groups due to the adsorption of atmospheric carbon dioxide during the synthesize of tri-metal composite (Xiang et al., 2014).

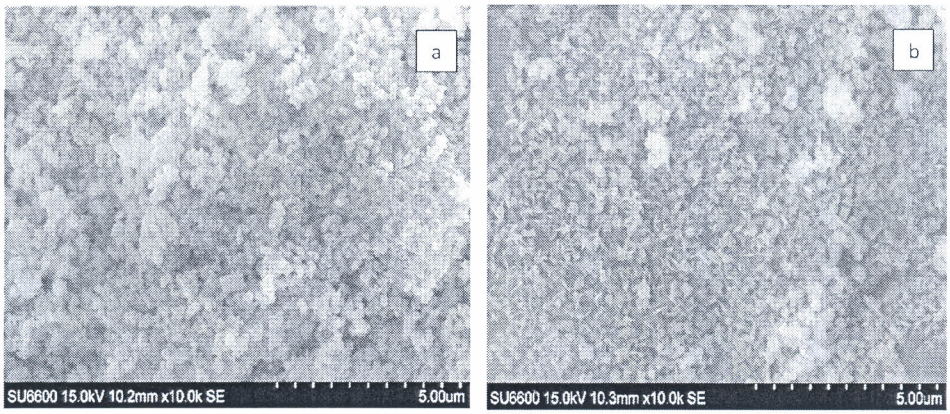


Fig. 4. SEM images of Fe-La-Ce tri-metal adsorbent a) before fluoride adsorption and b) after fluoride adsorption.

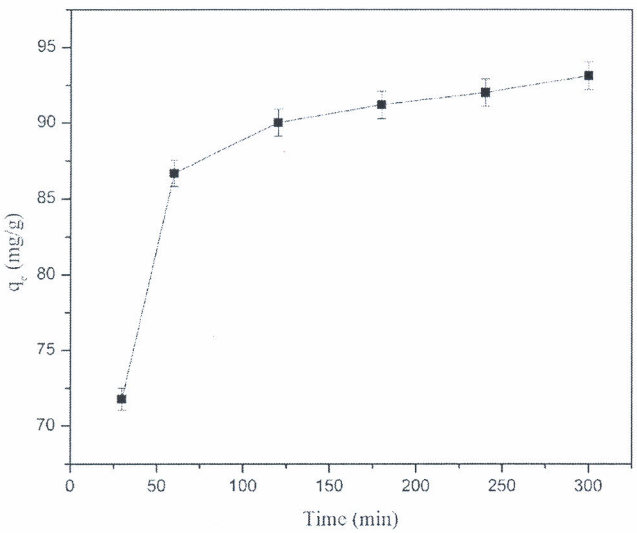


Fig. 5. The effect of contact time for fluoride ions adsorption onto Fe-La-Ce tri-metallic composite at 300 K. Adsorbent dose of 0.1 g/L and 10 mg/L of initial fluoride concentration were used at pH 7.0.

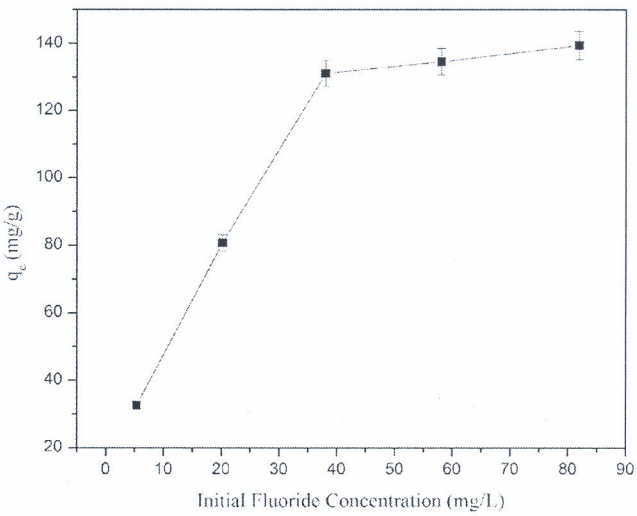


Fig. 6. The effect of initial fluoride concentration for fluoride ions adsorption process at 300 K. Adsorbent dose of 0.1 g/L was used at pH 7.0 for different fluoride concentrations.

The absorption band around 1118 cm^{-1} is attributed to sulphate groups (Topalian et al., 2013). The broad peaks around 3335 cm^{-1} and 1118 cm^{-1} demonstrated the presence of hydroxyl and sulphate groups in the newly synthesized tri-metal composite adsorbent (Dou et al., 2011). The broad peaks of virgin adsorbent around 3335.26 cm^{-1} and 1118.49 cm^{-1} were shifted to 3247.84 cm^{-1} and 1124.61 cm^{-1} respectively upon fluoride adsorption onto the tri-metallic composite. In addition, after fluoride adsorbed onto the adsorbate, intensities of the peaks around 3335.26 cm^{-1}, 1489.25 cm^{-1} and 1118.49 cm^{-1} have shown a significant decrease. By comparing the FTIR spectra, it can be concluded that hydroxides, carbonates, and sulphates were mainly contributing to the fluoride adsorption of the novel composite.

3.1.2. X-ray diffraction (XRD)

During the co-precipitation at basic pH conditions, all three metals were precipitated as their hydroxides. X-ray diffraction was carried out to confirm their presence in the tri-metal composite. X-ray peak analysis of a mixture of metal compounds is a challenging task. In addition, starting materials of tri-metal composite were not in pristine crystalline form. In order to overcome those challenges

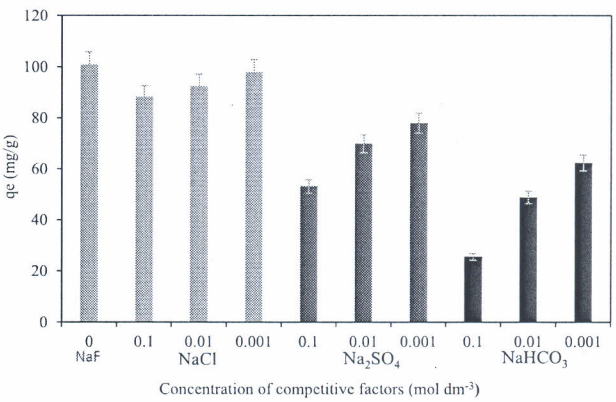


Fig. 7. Fluoride adsorption capacity of Fe-La-Ce tri-metal adsorbent in the presence of interfering anions at 300 K. Adsorbent dose of 0.1 g/L and 10.76 mg/L of initial fluoride concentration were used at pH 7.0.

during the characterization, XRD patterns of the individual metal hydroxides were separately obtained and compared those with the XRD peak positions of the metal compounds in the composite

Table 2
Percent interference from chloride, sulphate and bicarbonate ions for the fluoride adsorption capacity of the tri-metal composite at 300 K and pH 7.0.

Concentration of interfering ions/mol dm^{-3}	% interference from Chlorides	% interference from Sulphates	% interference from bicarbonate
0.100	12.51	47.25	74.64
0.010	8.24	30.63	51.51
0.001	2.86	22.64	38.13

Table 3
Fluoride removal efficiency of Fe-Ce-La tri-metal composite in natural water samples.

Sample no.	Fluoride concentration (mg/L)	pH	Conductivity (μScm^{-1})	*qe* (mg/g)
1	10.06	6.4	31.1	64.4
2	9.89	6.9	37.8	53.6
3	10.13	7.0	37.7	64.8
4	9.87	5.5	80.9	65.1
5	10.08	7.2	113.0	57.4

sample. Comparison of XRD patterns of the individual metal compounds and the tri-metal composites are shown in Fig. 2. Most of the X-ray diffraction lines observed for the tri-metal composites are corresponding to the diffraction lines of the individual metal hydroxides, which confirms that the individual metals are in their hydroxide forms in the composite sample.

Comparison of XRD patterns of trimetal composites before and after exposed to fluoride solution for 2 h are shown in Fig. 3. XRD patterns of the virgin tri-metal composite and the tri-metals treated with fluorides have identical diffraction patterns, which indicate that the fluoride adsorption had minimal effect on the mode of assembly of metals in the tri-metallic composite. This confirms the potential of using the tri-metal composites as a fluoride removing agent with minimal interference from the medium and fluoride adsorbed onto adsorbate is a physisorption process that involves electro statistic attraction coupled with possible ion exchanges.

3.1.3. *X-ray fluorescence*

The resulting peak characteristics of X-ray fluorescence are given in Table 1. The XRF analysis has confirmed that the synthesized composite contains all three metals in almost equal molecular compositions as expected from the co-precipitation procedure. The tri-metal adsorbents that were exposed to fluoride solutions were also characterized with XRF. In this study, these tri-metal adsorbents were introduced into the aqueous fluoride solution and stirred vigorously. Resulting metal compositions were almost identical to that of the pristine absorbent. Minute changes in the metal compositions in adsorbent before and after exposing to aqueous medium are due to the inherent composition variations in the co-precipitation method. These results substantiated the steadiness of the tri-metal adsorbent against dissolving in the aqueous environment. The pertinent peak analysis is given in Table 1.

3.1.4. *Scanning electron microscopic images*

Scanning electron micrographs of the Fe-La-Ce tri-metal adsorbent before and after fluoride adsorption are shown in Fig. 4. There are significant transformations in the surface morphology of the adsorbent before and after adsorption of fluorides ions. The granular shaped assemblies on the adsorbent surface had been transformed into sharped edged structures after soaked in fluoride solution. However, no composition changes were observed from XRF and XRD studies.

3.1.5. *Effect of contact time*

According to the experimental results shown in Fig. 5, the adsorption capacity was rapidly increased during the first hour due to the high amount of active sites available in the surface of the adsorbent, and then the increments were gradual because the adsorption process reaches to equilibrium. Even-though the adsorption capacity increases slowly with increasing contact time, longer contact times are not favorable for practical purposes. It was assumed that the equilibrium between adsorption processes has been reached within two hours of contact time. Therefore, the optimum contact time was regarded as two (02) hours.

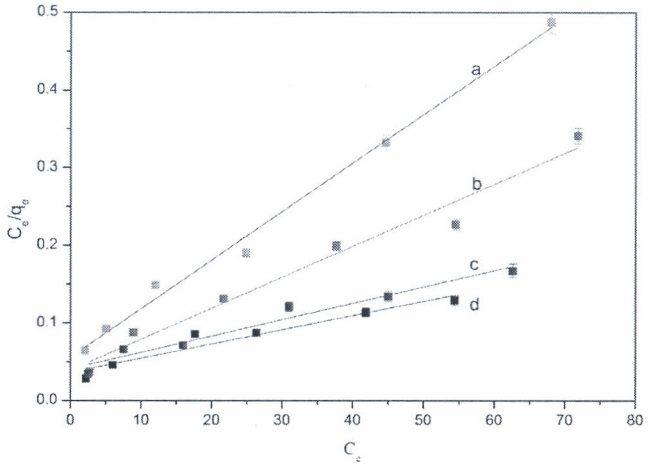


Fig. 8. Langmuir adsorption isotherm for the fluoride adsorption onto adsorbate at a) 301 K, b). 310 K, c). 320 K and d). 330 K.

Table 4
The summary of adsorbent isotherms.

pH	Temperature/K	Langmuir isotherm			Freundlich isotherm		
		Parameters					
		q_{max}	R^2	K_L	K_f	(1/n)	R^2
4.00	301	303.03	0.99	0.25	97.96	0.28	0.88
7.00	301	161.29	0.99	0.11	30.76	0.46	0.82
7.00	310	250.00	0.97	0.10	49.77	0.37	0.96
7.00	320	476.19	0.96	0.05	45.19	0.52	0.98
7.00	330	555.55	0.93	0.04	50.51	0.53	0.99

3.1.6. *Effect of pH*

It was observed that the adsorption capacity of the tri-metal adsorbent is significantly influenced by the pH of the medium

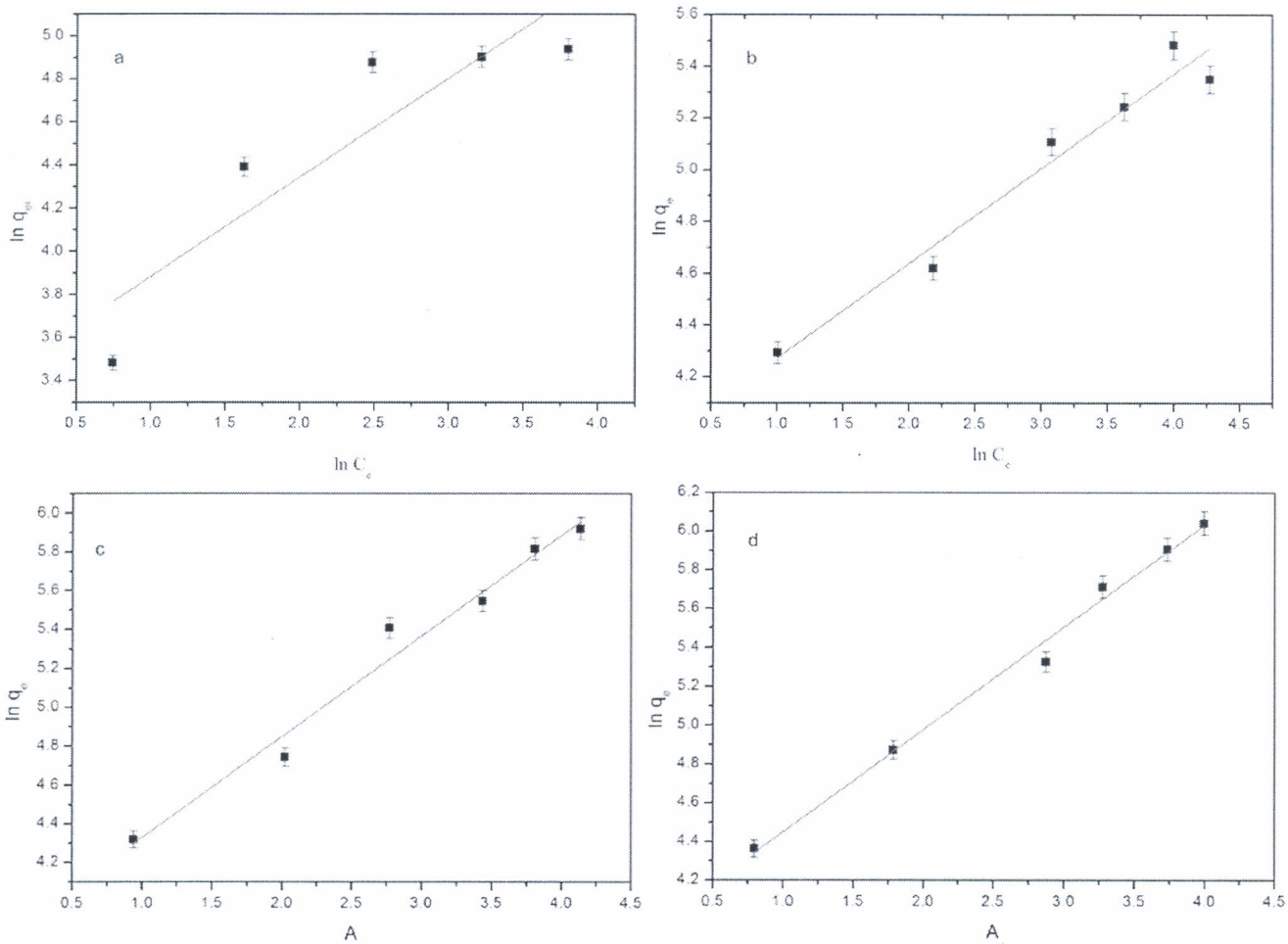


Fig. 9. Freundlich adsorption isotherm for the fluoride adsorption onto adsorbate at a) 300 K b) 310 K c) 320 K and d) 330 K.

Table 5
The summery of Dimensionless index at different temperatures and pH 7.00.

C_0 (mg/L)	R_L			
	301 K	310 K	320 K	330 K
10	0.47	0.50	0.66	0.71
20	0.31	0.33	0.50	0.55
50	0.15	0.16	0.28	0.29

Table 6
Fluoride adsorption capacities at different adsorbents.

Adsorbent	pH	q_{max} (mg/g)	Reference
Fe-Al-Ce	7.0	2.22	(Chen et al., 2009)
Fe-Mg-La	7.0	185.2	(Yu et al., 2015a)
	4.0	270.3	
Mg-La-Ce	7.0	37.43	(Wu et al., 2016)
Fe-Zr	6.8	8.21	(Biswas et al., 2007)
Ca-Al-La	6.8	29.30	(Xiang et al., 2014)
Fe-Mg-Al	6.0	14.92	(Ma et al., 2011)
Fe-La-Ce	7.0	161.29	Present work
	4.0	303.03	

where fluoride adsorption capacity decreases considerably with increasing alkalinity of the medium as shown in Fig. 1a in the supporting information. The highest adsorption capacity of 305.81 mg/g was achieved at pH of 4.0. The point of zero charge (pH_{pzc}) in this experiment was 7.27. The medium pH was lower than pH_{pzc}, and hence the adsorbent was in its protonated form.

At pH < pH_{pzc} two processes are possible. First, the active sites of the adsorbent (specially OH ions) (Biswas et al., 2009) can be protonated leading to a better interaction between negatively charged fluoride ions with the positively charged Fe-La-Ce tri-metallic adsorbent. On the other hand, fluoride ions get protonated to produce HF (pKa 2.95) (Mohapatra et al., 2012) under strongly acidic conditions. The mode of interaction between the adsorbent or protonated adsorbent and the fluoride ions (F^-) could be different to that of hydrofluoric acid (HF). In any case, the adsorption capacity is better in the acidic media.

At the medium pH higher than the point of zero charge (pH_{pzc} = 7.27), tri-metallic composite has an overall negative charge. The adsorption capacity of trimetal composites decreases at pH > pH_{pzc} due to electro statistic repulsion between tri-metallic composite to negatively charged fluoride ions. Also, hydroxide ions out-compete fluoride ions for active sites on the adsorbent. Even though a considerably small amount of fluoride ions were adsorbed at high alkaline medium due to ion-exchange mechanism and non-specific electro-statistic attractions (Yang et al., 2011).

3.1.7. *Effect of initial concentration*

The adsorption capacity increased until the initial fluoride

UNIVERSITY OF SRI JAYEWARDENEPURA
16 FEB 2018

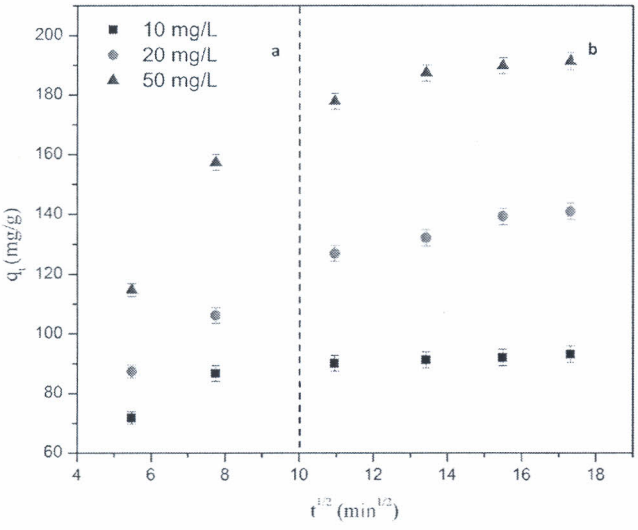


Fig. 10. Fluoride adsorption data fitted to intra-particle diffusion model.

concentration was reached to 40 mg/L at 300 K for 0.1 g/L adsorbent dose and thereafter, the adsorption capacity remained fairly constant while increasing fluoride concentration as shown in Fig. 6. According to the given experimental conditions it could be assumed that the most efficient fluoride removal capacity can be achieved when the initial fluoride concentration of the test solutions is 40 mg/L or above for 0.1 g/L of tri-metal composite.

3.1.8. The effect of competition of interfering anions

The effect of competition of interfering anions that are commonly present in natural waters for the fluoride adsorption by Fe-La-Ce tri-metal was studied. Fig. 7 shows the fluoride adsorption capacity of tri-metal composite in the presence of chloride, sulphate and bicarbonate ions at different initial concentrations. The minimal interference for the fluoride adsorption was observed from chloride ions and a significant interference was observed from bicarbonate ions (Platikanov et al., 2017). Interference from sulfates to removal of fluoride ions is at a moderate level. Percentage interferences from these inferring anions to the fluoride adsorption process were calculated using equation (3). Tabulated percentage interferences are tabulated in Table 2.

$$\text{Interference } \% = \frac{q_{wo} - q_w}{q_{wo}} \times 100\% \tag{3}$$

q_{wo} = fluoride adsorption capacity of the composite in the absence interfering ions

q_w = fluoride adsorption capacity of the composite in the presence interfering ions

3.1.8.1. Applicability of Fe-La-Ce tri-metal composite for treat natural water samples. Applicability of Fe-Ce-La tri-metal composite was tested using natural water samples collected from different geographical regions (Polonnaruwa, Anuradhapura, Kandy, Hambantota, Galle and Matara) of Sri Lanka. Since initial fluoride ion concentrations of the aforementioned samples were in the range of 0.5–1.5 mg/L, 10 mg/g of final fluoride ion concentration was maintained to check the efficiency of the tri-metal composite. Collected natural water samples have shown different conductivities due to their total dissolved ionic species presence in water. The summary of the removal behavior of fluoride ions in four natural water samples are shown in Table 3. These results have confirmed that the above sample matrices have a minimal influence on fluoride adsorption capacity of Fe-Ce-La tri-metal composite.

3.1.9. Adsorption isotherms of fluoride/tri-metal composite system

Adsorption between fluoride ions and adsorbate is governed by the strength of the complexation of fluorides with metal ions. Such adsorption can be best described by monolayer adsorption due to better interactions between adsorbent and the adsorbate, over the intermolecular interactions among fluoride ions. Therefore, the adsorption behavior of fluorides to tri-metal composite was studied using Langmuir and Freundlich adsorption isotherms. The Langmuir adsorption isotherm seemed valid only for monolayer adsorption onto a finite number of identical active sites that containing on adsorbent surface (Mohan and Karthikeyan, 1997). The Langmuir adsorption isotherm equation is portrayed as;

$$\frac{C_e}{q_e} = \frac{1}{K_L q_{max}} + \frac{C_e}{q_{max}} \tag{4}$$

In the case of q_e being the weight of fluoride ions adsorbed per unit weight of adsorbent (in mg/g) at the equilibrium, C_e is the equilibrium concentration of fluoride ions (in mg/L), K_L is the Langmuir constant, and q_{max} is the maximum adsorption capacity of tri-metal for fluoride ions.

Adsorption data of fluoride/tri-metal system were quantified from the fluoride ion sensitive electrode method as described previously and measurements were triplicated. The resulting data were fitted to equation (4) and the corresponding regressions as a function of temperature are shown in Fig. 8. Linear regressions were observed with R^2 values over 0.99, which substantiate the hypothesis of monolayer formation of Fluoride ions on Fe-La-Ce tri-metal surface. At relatively higher temperatures, K_L shifted to lower values by forming incomplete monolayers on tri-metal surface under the provided concentration conditions. This confirms that the physisorption process and the reversibility of the fluoride adsorption process. Relevant q_{max} and K_L for different temperatures are summarized in Table 4.

Fluoride adsorption data of the tri-metal composites were also analyzed according to the Freundlich adsorption isotherm (Dada et al., 2012), which is shown in equation (5). In the Freundlich model K_F represents the adsorption capacity and $1/n$ is the adsorption intensity. Data were modeled to the Freundlich isotherm and are shown in Fig. 9. At 301 K, data were poorly behaved according to the model. However, statistics of the regression lines were improved for the data at elevated temperatures. As shown in Table 4, adsorption intensities (1/n) obtained for fluoride adsorption data are varying in between 0.2 and 0.5 for different temperatures. This confirms the heterogeneous nature of the fluoride adsorption sites on the tri-metal surface, where more than one metal is involved in the fluoride chelating process.

$$\ln q_e = \frac{1}{n} \ln C_e + \ln K_F \tag{5}$$

The feasibility of the interaction was explained using dimensionless adsorption intensity (R_L), which is shown in equation (6). Considering the R_L values (Gayani et al., 2017; Weber and Chakravorti, 1974), $R_L > 1$ for unfavorable, $R_L = 1$ for linear and $R_L < 1$ for favorable for fluoride ions adsorbed onto adsorbate and reversible reaction possible when $R_L < 1$.

$$R_L = \frac{1}{1 + K_L C_0} \tag{6}$$

Table 7
The summery of fluoride adsorption kinetic data at 300 K and pH 7.00.

Kinetic model	Kinetic parameters		
	C_i (mg/L)		
	10 mg/L	20 mg/L	50 mg/L
Pseudo-first-order rate model	q_e = 1.15 mg/g $K_1 = 6.90 \times 10^{-4}$ min^{-1} R^2 = 0.5767	q_e = 1.35 mg/g $K_1 = 1.61 \times 10^{-3}$ min^{-1} R^2 = 0.7995	q_e = 1.19 mg/g $K_1 = 1.61 \times 10^{-4}$ min^{-1} R^2 = 0.6534
Pseudo-second-order rate model	q_e = 95.42 mg/g $K_2 = 1.30 \times 10^{-3}$ g/mg min R^2 = 0.9998	q_e = 153.85 mg/g $K_2 = 2.60 \times 10^{-4}$ g/mg min R^2 = 0.9995	q_e = 205.76 mg/g $K_2 = 2.40 \times 10^{-4}$ g/mg min R^2 = 0.9993
Intra particle diffusion model	k_{id} = 1.48 mg g^{-1} $min^{-1/2}$ C = 70.03 mg g^{-1} R^2 = 0.7162	k_{id} = 4.47 mg g^{-1} $min^{-1/2}$ C = 69.69 mg g^{-1} R^2 = 0.9282	k_{id} = 5.90 mg g^{-1} $min^{-1/2}$ C = 100.39 mg g^{-1} R^2 = 0.8179

Table 8
Summery of regeneration ability for removal of fluoride ions at pH 10.

Number of regeneration cycle	Adsorption capacity (mg/g)	Desorption capacity (mg/g)	Percentage of desorption (%)
1	87.45	84.07	96.13
2	79.42	73.50	92.54
3	70.51	63.17	89.59

In equation (6), C_0 is the initial concentration (mg/L) of fluoride ions and K_L is Langmuir constant. These adsorption intensity data are shown in Table 5.

According to the above data, the value of R_L decreased when the concentration of fluoride solutions was increased. In addition, they were increased slowly when temperature increased but did not go above 1. Therefore, it indicates that the Langmuir isotherm is favorable for fluoride ions adsorbed onto Fe-La-Ce tri-metallic composite. Low values of R_L describes that fluoride ions adsorption onto Fe-La-Ce tri-metallic composite is a physical and reversible process.

A comparison of the maximum adsorption capacities for different literature reported metal composites are summarized in Table 6.

3.1.10. Adsorption kinetics

Kinetics of fluoride adsorption onto Fe-La-Ce tri-metal adsorbent was followed to study the fluoride removing rates and potential adsorption mechanism. In this respect, pseudo 1st and 2nd order kinetics were followed, and the corresponding kinetic equation are given in equations (7) and (8) respectively.

$$\log\ (q_e - q_t) = \log(q_e) - \frac{k_1}{2.303} t \tag{7}$$

$$\frac{t}{q_t} = \frac{1}{k_2 q_e^2} + \frac{1}{q_e} t \tag{8}$$

In above equations, q_t is the amount of Fluoride ions removed at time t (mg/g), q_e is the adsorption capacity at the equilibrium (mg/g), k_1 and k_2 are the pseudo-first and pseudo-second order rate constants respectively.

Using equation (7), log $(q_e - q_t)$ versus t was plotted to compare adsorption kinetic with the pseudo-first order rate law (Reddad et al., 2002). Subsequent data analysis has shown a poor agreement of fluoride adsorption data to pseudo-first order kinetics as shown in Fig. 2 in supporting information. Because experimental q_{max} (161.29 mg/g) and calculated q_{max} (1.15 mg/g) didn't agreed and also correlation coefficient was very poor (R^2 = 0.5767) at pH 7.0 and 28 °C. Therefore, kinetic data were then analyzed to the pseudo-second order rate lay by plotting t/q_t vs t (Ho and McKay, 1999). As shown in Fig. 3 in supporting information, data are well behaved (R^2 of 0.99) with the pseudo-second-order rate model. The Resulting pseudo-second order rate constants for different initial fluoride concentrations differ very closely in the average of 0.0005 g/mg min.

The Intra particle diffusion rate model was used to predict the mechanism of fluoride ions adsorption onto Fe-La-Ce tri-metallic composites (Mckay et al., 1983). The Adsorption kinetic of the above model was calculated using equation (9).

$$q_t = k_{id}\sqrt{t} + C \tag{9}$$

In equation (9), K_{id} remains the intra particle diffusion constant (its units in mg/g $min^{-1/2}$), C is a constant and it is important to determine boundary layer effect. $C = 0$ indicates that adsorption process is controlled only by the intra particle diffusion model. $C \neq 0$ indicated that the adsorption process is complicated. The adsorption process does not only involve the intra particle diffusion model but also other kinetic models are involved (Wang et al., 2014). As shown in Fig. 10, two distinguished linear sections (a and b) were identified. It causes due to external mass transfer and the inter particle diffusion model (Ho et al., 2000). Therefore, fluoride ions adsorption is a complicated process (Fan et al., 2012), which is a combination of intra particle diffusion rate model and an external mass transfer process. A summary of fluoride adsorption kinetics data for above 3 models are given in Table 7.

3.1.11. Regeneration

Fluoride adsorb onto tri-metallic composite is highly dependent on pH. Poor adsorption capacity shows at high pH values (more than pH 10). Therefore, a regeneration study was carried out at pH 10 using 1 M NaOH. The cyclic process of adsorption and desorption were studied and adsorption capacities were shown in Table 8. According to study, Fe-La-Ce tri-metallic composite exhibits excellent regeneration and reusability.

Overall, the high fluoride removal capacity of trimetal complex has been attributed to the reversible isomorphic substitution between F^- and OH^-. Therefore, pH is a crucial factor of deciding the maximum adsorption capacity of the composite. Based on the experimental results, fluoride removal from tri-metal composite is mainly governed by the ion exchange mechanism and have shown a better regeneration ability.

4. Conclusion

The Fe-La-Ce tri-metal composites have shown significantly high adsorption capacities (q_{max} is 303.03 mg/g and 161.29 mg/g at pH 4.00 and 7.00 respectively) towards the fluoride ions in aqueous systems. The Fluoride adsorption process onto the tri-metal have shown a pseudo-second order type adsorption kinetics and obeyed Langmuir type monolayer adsorption behavior. The minimal interference for the fluoride adsorption were observed from chloride ions and sulphate ions but significant interference was observed from bicarbonate ions. Fe-La-Ce composites can be introduced as a novel fluoride removing material, which efficiently removes fluoride ions when the pH of the medium is less than 7 and exhibits excellent regeneration (desorption percentage 96.13%) and reusability.

Acknowledgement

Financial support was provided by the University Research Grants (ASP/01/RE/SCI/2015/31, ASP/06/RE/SCI/2014/06 and ASP/01/RE/SCI/2015/29) at University of Sri Jayewardenepura, Sri Lanka. Advanced Material Research Center and Central Instrumentation Facility of University of Sri Jayewardenepura have facilitated the instrumental analysis for this study.

Appendix A. Supplementary data

Supplementary data related to this article can be found at https://doi.org/10.1016/j.jenvman.2017.11.041.

References

Bhatnagar, A., Kumar, E., Sillanpää, M., 2011. Fluoride removal from water by adsorption—a review. Chem. Eng. J. 171, 811–840.
Biswas, K., Bandhoyapadhyay, D., Ghosh, U.C., 2007. Adsorption kinetics of fluoride on iron (III)- zirconium (IV) hybrid oxide. Adsorption 13, 83–94.
Biswas, K., Gupta, K., Ghosh, U.C., 2009. Adsorption of fluoride by hydrous iron (III)—tin (IV) bimetal mixed oxide from the aqueous solutions. Chem. Eng. J. 149, 196–206.
Cai, H.-m., Chen, G.-j., Peng, C.-y., Zhang, Z.-z., Dong, Y.-y., Shang, G.-z., Zhu, X.-h., Gao, H.-j., Wan, X.-c., 2015. Removal of fluoride from drinking water using tea waste loaded with Al/Fe oxides: a novel, safe and efficient biosorbent. Appl. Surf. Sci. 328, 34–44.
Chen, L., Wu, H.-X., Wang, T.-J., Jin, Y., Zhang, Y., Dou, X.-M., 2009. Granulation of Fe—Al—Ce nano- adsorbent for fluoride removal from drinking water by spray coating on sand in a fluidized bed. Powder Technol. 193, 59–64.
Choi, S., Yun, Z., Hong, S., Ahn, K., 2001. The effect of co-existing ions and surface characteristics of nanomembranes on the removal of nitrate and fluoride. Desalination 133, 53–64.
Cristiano, E., Hu, Y.-J., Siegfried, M., Kaplan, D., Nitsche, H., 2011. A comparison of point of zero charge measurement methodology. Clays Clay Miner. 59, 107–115.
Dada, A., Olalekan, A., Olatunya, A., Dada, O., 2012. Langmuir, Freundlich, Temkin and Dubinin– Radushkevich isotherms studies of equilibrium sorption of Zn2 + unto phosphoric acid modified rice husk. IOSR J. Appl. Chem. 3, 38–45.
Daifullah, A., Yakout, S., Elreefy, S., 2007. Adsorption of fluoride in aqueous solutions using KMnO 4- modified activated carbon derived from steam pyrolysis of rice straw. J. Hazard Mater. 147, 633–643.
Dong, S., Wang, Y., 2016. Characterization and adsorption properties of a lanthanum-loaded magnetic carbonic hydrogel composite for fluoride removal. Water Res. 88, 852–860.
Dou, X., Zhang, Y., Zhao, B., Wu, X., Wu, Z., Yang, M., 2011. Arsenate adsorption on an Fe—Ce bimetal oxide adsorbent: EXAFS study and surface complexation modeling. Colloid. Surface. Physicochem. Eng. Aspect. 379, 109–115.
Ergun, E., Tor, A., Cengeloglu, Y., Kocak, I., 2008. Electrodialytic removal of fluoride from water: effects of process parameters and accompanying anions. Separ. Purif. Technol. 64, 147–153.
Fan, L., Luo, C., Li, X., Lu, F., Qiu, H., Sun, M., 2012. Fabrication of novel magnetic chitosan grafted with graphene oxide to enhance adsorption properties for methyl blue. J. Hazard Mater. 215, 272–279.
Favier, L., Simion, A.I., Matei, E., Cristina, C.G., Kadmi, Y., Bouzaza, A., 2016. Photocatalytic oxidation of a hazardous phenolic compound over TiO_2 in batch system. Environ. Eng. Manage. J. 15 (5), 1059–1067.
Ganvir, V., Das, K., 2011. Removal of fluoride from drinking water using aluminum hydroxide coated rice husk ash. J. Hazard Mater. 185, 1287–1294.
Gayani, B., Perera, A.D.L.C., Kottegoda, N., 2017. Thermodynamic, equilibrium and kinetic studies of adsorption of Rhodamine B onto activated bamboo carbon. Desalin. Water Treat. 67.
Gogoi, S., Nath, S.K., Bordoloi, S., Dutta, R.K., 2015. Fluoride removal from groundwater by limestone treatment in presence of phosphoric acid. J. Environ. Manag. 152, 132–139.
Güler, C., Thyne, G.D., 2004. Delineation of hydrochemical facies distribution in a regional groundwater system by means of fuzzy c-means clustering. Water Resour. Res. 40.
Ho, Y.-S., McKay, G., 1999. Pseudo-second order model for sorption processes. Process Biochem. 34, 451–465.
Ho, Y., Ng, J., McKay, G., 2000. Kinetics of pollutant sorption by biosorbents: review. Separ. Purif. Meth. 29, 189–232.
Ma, W., Zhao, N., Yang, G., Tian, L., Wang, R., 2011. Removal of fluoride ions from aqueous solution by the calcination product of Mg—Al—Fe hydrotalcite-like compound. Desalination 266, 20–26.
McKay, G., Blair, H., Gardner, J., 1983. The adsorption of dyes in chitin. III. Intraparticle diffusion processes. J. Appl. Polym. Sci. 28, 1767–1778.
Mohan, S.V., Karthikeyan, J., 1997. Removal of lignin and tannin colour from aqueous solution by adsorption onto activated charcoal. Environ. Pollut. 97, 183–187.
Mohapatra, M., Hariprasad, D., Mohapatra, L., Anand, S., Mishra, B., 2012. Mg-doped nano ferrihydrite—a new adsorbent for fluoride removal from aqueous solutions. Appl. Surf. Sci. 258, 4228–4236.
Naim, M.M., Moneer, A.A., El-Said, G.F., 2012. Defluoridation of commercial and analar sodium fluoride solutions without using additives by batch electrocoagulation-flotation technique. Desalin. Water Treat. 44, 110–117.
Noorjahan, M., Khayyum, M., Mangatayaru, K.G., 2015. A novel cobalt modified layered double hydroxide for the efficient removal of fluoride. Mater. Focus 4, 283–289.
Oshima, K., Evans-Strickfaden, T., Highsmith, A., Ades, E., 1996. The use of a microporous polyvinylidene fluoride (PVDF) membrane filter to separate contaminating viral particles from biologically important proteins. Biologicals 24, 137–145.
Platikanov, S., Hernandez, A., Gonzalez, S., Cortina, J.L., Tauler, R., Devesa, R., 2017. Predicting consumer preferences for mineral composition of bottled and tap water. Talanta 162, 1–9.
Prabhu, S.M., Meenakshi, S., 2015. Defluoridation of water using synthesized Zr (IV) encapsulated silica gel/chitosan biocomposite: adsorption isotherms and kinetic studies. Desalin. Water Treat. 53, 3592–3603.
Rafique, A., Awan, M.A., Wasti, A., Qazi, I.A., Arshad, M., 2012. Removal of fluoride from drinking water using modified immobilized activated alumina. J. Chem. 2013.
Rafique, A., Awan, M.A., Wasti, A., Qazi, I.A., Arshad, M., 2013. Removal of fluoride from drinking water using modified immobilized activated alumina. J. Chem. 2013, 1–7.
Reddad, Z., Gerente, C., Andres, Y., Le Cloirec, P., 2002. Adsorption of several metal ions onto a low-cost biosorbent: kinetic and equilibrium studies. Environ. Sci. Technol. 36, 2067–2073.
Selm, P., 2008. Fluoride removal with extra low energy reverse osmosis membranes: three years of large scale field experience in Finland. Desalination 223, 73–84.
Topalian, Z., Stefanov, B., Granqvist, C.-G., Österlund, L., 2013. Adsorption and photooxidation of acetaldehyde on TiO 2 and sulfate-modified TiO 2: studies by in situ FTIR spectroscopy and micro-kinetic modeling. J. Catal. 307, 265–274.
Tor, A., 2006. Removal of fluoride from an aqueous solution by using montmorillonite. Desalination 201, 267–276.
Turner, B.D., Binning, P., Stipp, S., 2005. Fluoride removal by calcite: evidence for fluorite precipitation and surface adsorption. Environ. Sci. Technol. 39, 9561–9568.
Wang, P., Cao, M., Wang, C., Ao, Y., Hou, J., Qian, J., 2014. Kinetics and thermodynamics of adsorption of methylene blue by a magnetic graphene-carbon nanotube composite. Appl. Surf. Sci. 290, 116–124.
Weber, T.W., Chakravorti, R.K., 1974. Pore and solid diffusion models for fixed-bed adsorbers. AIChE J. 20, 228–238.
Wei, C., Guo, H., Zhang, D., Wu, Y., Han, S., An, Y., Zhang, F., 2016. Occurrence and hydrogeochemical characteristics of high-fluoride groundwater in Xiji County, southern part of Ningxia Province, China. Environ. Geochem. Health 38, 275–290.
Wu, L., Zhang, G., Tang, D., 2016. A novel high efficient Mg—Ce—La adsorbent for fluoride removal: kinetics, thermodynamics and reusability. Desalin. Water Treat. 1–12.
Xiang, W., Zhang, G., Zhang, Y., Tang, D., Wang, J., 2014. Synthesis and characterization of cotton-like Ca—Al—La composite as an adsorbent for fluoride removal. Chem. Eng. J. 250, 423–430.
Yang, S.-T., Chen, S., Chang, Y., Cao, A., Liu, Y., Wang, H., 2011. Removal of methylene blue from aqueous solution by graphene oxide. J. Colloid Interface Sci. 359, 24–29.
Yu, Y., Yu, L., Chen, J.P., 2015a. Adsorption of fluoride by Fe–Mg–La triple-metal composite: adsorbent preparation, illustration of performance and study of mechanisms. Chem. Eng. J. 262, 839–846.
Yu, Y., Yu, L., Paul Chen, J., 2015b. Adsorption of fluoride by Fe—Mg—La triple-metal composite: adsorbent preparation, illustration of performance and study of mechanisms. Chem. Eng. J. 262, 839–846.
Zhang, Y., Yang, M., Dou, X.-M., He, H., Wang, D.-S., 2005. Arsenate adsorption on an Fe-Ce bimetal oxide adsorbent: role of surface properties. Environ. Sci. Technol. 39, 7246–7253.